Theoretical Kinetics Study of the O(P−3) + CH4/CD4 Hydrogen Abstraction Reaction: The Role of Anharmonicity, Recrossing Effects, and Quantum Mechanical Tunneling

ARTICLE *in* THE JOURNAL OF PHYSICAL CHEMISTRY A · APRIL 2014

Impact Factor: 2.69 · DOI: 10.1021/jp5028965 · Source: PubMed

THE JOURNAL OF PHYSICAL CHEMISTRY A

Article

pubs.acs.org/JPCA

Theoretical Kinetics Study of the $O(^3P) + CH_4/CD_4$ Hydrogen Abstraction Reaction: The Role of Anharmonicity, Recrossing Effects, and Quantum Mechanical Tunneling

Eloisa Gonzalez-Lavado,[†] Jose C. Corchado,[†] Yury V. Suleimanov,*[,‡,§] William H. Green,[‡] and Joaquin Espinosa-Garcia*[,†]

[†]Departamento de Química Física, Universidad de Extremadura, 06071 Badajoz, Spain

[‡]Department of Chemical Engineering, Massachusetts Institute of Technology, 77 Massachusetts Avenue, Cambridge, Massachusetts 02139, United States

[§]Department of Mechanical and Aerospace Engineering, Combustion Energy Frontier Research Center, Princeton University, Olden Street, Princeton, New Jersey 08544, United States

ABSTRACT: Using a recently developed full-dimensional accurate analytical potential energy surface [Gonzalez-Lavado, E.; Corchado, J. C.; Espinosa-Garcia, J. *J. Chem. Phys.* **2014**, *140*, 064310], we investigate the thermal rate coefficients of the $O(^3P) + CH_4/CD_4$ reactions with ring polymer molecular dynamics (RPMD) and with variational transition-state theory with multidimensional tunneling corrections (VTST/MT). The results of the present calculations are compared with available experimental data for a wide temperature range 200−2500 K. In the classical high-temperature limit, the RPMD results match perfectly the experimental data, whereas VTST results are smaller by a factor of 2. We suggest that this discrepancy is due to the harmonic approximation used in the present VTST calculations, which leads to an overestimation of the variational effects. At low temperatures the tunneling plays an important role, which is captured by both methods, although they both overestimate the experimental values. The analysis of the kinetic isotope effects shows a discrepancy between both approaches, with the VTST values smaller by a factor about 2 at very low temperatures. Unfortunately, no experimental results are available to shed any light on this comparison, which keeps it as an open question.

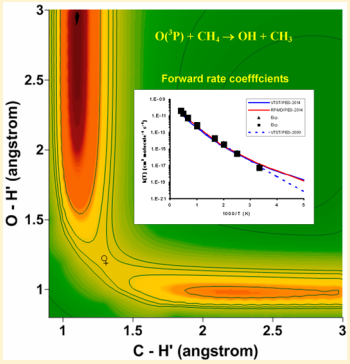

1. INTRODUCTION

Ground-state oxygen atom chemistry is of great importance over a wide temperature and energy range. The title reaction, $O(^3P) + CH_4$, is important for hydrocarbon combustion and it is also a prototypical reaction for oxygen−hydrocarbon combustion. At high temperatures (1000−2500 K), because of heavy-light-heavy mass combination, many recrossings of the dividing surface separating reactants from products are expected. At low temperatures (200−300 K), because of light hydrogen atom transfer this reaction is also a good candidate to study quantum tunneling effects. Moreover, at very high energies (2−5 eV) it is an important step in the mechanism of polymer hydrocarbon decomposition in low Earth orbit (LEO).

The thermal rate coefficients of the reaction with methane, $O(^3P) + CH_4 \rightarrow OH + CH_3$, have been measured experimentally with a wide variety of methods.[1−21] The most recent recommended expression for the rate coefficients for the temperature range 300−2500 K is[21]

$$k(T) = 1.15 \times 10^{-15} T^{1.56} \exp(-4270/T)\ \text{cm}^3\ \text{molecule}^{-1}\ \text{s}^{-1} \quad (1)$$

although below 400 K, the value of $k(T)$ is considerably less reliable due to the uncertainties in the reaction stoichiometry,[18] and possibly large tunneling effects. In addition, expression 1 gives low-temperature rate coefficients lower than most of the experimental results, and Cohen[18] proposed an alternative expression of the experimental results given by

$$k(T) = 2.69 \times 10^{-18} T^{2.3} \exp(-3570/T)\ \text{cm}^3\ \text{molecule}^{-1}\ \text{s}^{-1} \quad (2)$$

Equation 2 leads to higher values of the rate coefficient than eq 1 at low temperatures (up to 60% higher at 300 K), in better agreement with the experimental values.

The kinetics of this reaction has also received great theoretical attention.[22−29] In 1988 some of us[22] studied the kinetics of this reaction using variational transition-state theory (VTST) in curvilinear coordinates with transmission coefficients calculated by the microcanonical optimized multidimensional tunneling approximation[22] (VTST/MT), where a dual-level algorithm was used for the dynamical calculations. Good agreement with experiment was obtained. In that work we developed the first analytical potential energy surface, which was, however, not symmetric with respect to the permutation of the four hydrogens. On the basis of this surface, Clary[23]

Received: March 24, 2014
Revised: April 21, 2014
Published: April 21, 2014

performed time-independent quantum scattering calculations, obtaining rate coefficients lower than the experimental values. To improve the deficiencies of the earlier surface, in 2000 our group[24] reported a new analytical surface for the title reaction (PES-2000), which was symmetric with respect to any permutation of the four methane hydrogens. Using this surface, the thermal rate coefficients of this reaction have been calculated using different approaches: variational transition-state theory with multidimensional tunneling (VTST/MT),[24] multiconfiguration time-dependent Hartree (MCTDH),[25] quasi-classical trajectory (QCT),[26] reduced-dimensional quantum dynamics (QD),[27,28] and more recently ring polymer molecular dynamics (RPMD),[29] yielded in general good agreement with the experimental data. In this last paper, the authors noted, however, that it is possible that this PES-2000 is still not sufficiently accurate. For example, the PES has a barrier height of 13.0 kcal mol^{-1} and an imaginary frequency of 1549 cm^{-1} at the transition state, which is significantly smaller than the ab initio values, 14.0 kcal mol^{-1} and about 2000 cm^{-1}, respectively. So, a thinner barrier might facilitate more facile tunneling. To correct the deficiencies of PES-2000, recently our lab reported the construction of a new analytical surface for the title reaction based *exclusively* on high-level ab initio calculations, denominated as PES-2014.[30] An advantage of this surface is that not only the energy is obtained analytically but also the first energy derivatives, i.e., the gradients, which is a very desirable feature in kinetics and dynamics calculations.

In addition, this reaction also represents a theoretical challenge because the approach of $O(^3P)$ along a CH bond has 3-fold symmetry and leads to a Jahn−Teller conical intersection rather than a saddle point. The conical intersection corresponds to a ^3E state, and breaking the C_{3v} symmetry splits this into two surfaces, $^3A'$ and $^3A''$. Walch and Dunning[31] and Schlegel et al.[32] using ab initio molecular orbital calculations, obtained the optimized geometries and frequencies at the stationary points, and the barrier height and heat of reaction. The saddle point geometry is found to be of C_s symmetry, but close to C_{3v}, and the predicted barrier heights for the two surfaces ($^3A'$ and $^3A''$) present a very small difference (0.2 kcal mol^{-1}).

The title reaction is a hydrogen abstraction reaction, which is affected by quantum effects, such as zero-point energy (ZPE) and tunneling, and recrossing. Theoretically, the accuracy of the kinetics (and also dynamics) description of a chemical reaction depends mainly on two factors: the kinetics (dynamics) approach and the potential energy surface (PES). Accurate thermal rate coefficients only could be obtained using exact quantum mechanical methods (based on accurate surfaces), which is usually very difficult for full-dimensional polyatomic systems. Different approaches have been proposed to circumvent this problem, and in the present paper we analyze two approaches: variational transition-state theory with multidimensional tunneling effect (VTST/MT) and ring polymer molecular dynamics (RPMD), which take into account the quantum effects (tunneling and ZPE) and recrossing in different ways. First, at low temperatures, whereas in the first one (VTST/MT) the tunneling is included as a semiclassical correction factor to the short-time limit of the classical real-time correlation functions calculated using quantum partition functions, in the second one (RPMD) its path integral nature allows the inclusion of quantum tunneling effect through a connection between RPMD and semiclassical instanton theory[33] and ZPE effect due to rigorous treatment of the quantum Boltzmann operator.[34] Second, at high temperatures, whereas the first one reduces the recrossing by variational optimization of the dividing surface, the RPMD rate theory treats recrossing more explicitly by analyzing the long-time limit of the corresponding real-time correlation functions.[34] Note that both VTST and RPMD approaches assume Boltzmann equilibrium of energy levels, i.e., high-pressure limit.

In summary, the main aim of the present paper is to analyze various effects that affect the calculations of the thermal rate coefficients using two dynamics approaches. The article is structured as follows. In section 2, a brief description of the PES-2014 is presented. In section 3, we briefly outline some computational details of the kinetics calculations. The results are presented and compared with the available experimental data in section 4. Finally, section 5 contains the conclusions.

2. POTENTIAL ENERGY SURFACE

The PES-2014 has been exhaustively described in an earlier paper,[30] and here it will be briefly outlined. Basically, it consists of four LEP-type (London−Eyring−Polanyi) stretching terms, valence (val) bending terms for each bond angle in methane, quadratic-quartic terms whose aim is to correctly describe the out-of-plane motion of methyl, and a van der Waals term to describe the intermediate complexes in the entrance and exit channels. In addition, it includes a series of switching functions allowing the smooth change from pyramidal CH_4 to planar CH_3 product. It depends on 41 adjustable parameters, which are fitted to very high-level ab initio calculations, CCSD(T) = FULL/aug-cc-pVQZ. This surface presents a barrier height of 14.1 kcal mol^{-1} and reaction energy of 5.8 kcal mol^{-1}, reproducing benchmark calculations.[35] In addition, it presents intermediate complexes in the entrance and exit channels. For the sake of clarity, Figure 1 plots schematically the variations in potential energy along the hydrogen abstraction reaction path for the PES-2014.

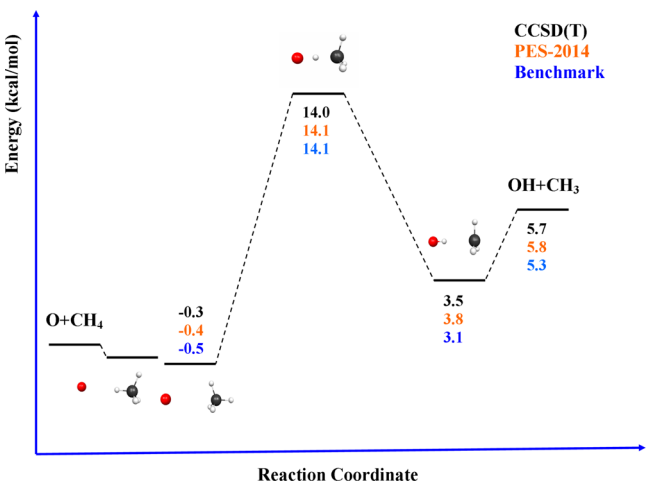

Figure 1. Schematic profile of the potential energy surface along the reaction path. CCSD(T): CCSD(T)=FULL/aug-cc-pVQZ//CCSD-(T)=FC/cc-pVTZ single point level from ref 30. PES-2014: using the analytical surface developed ref 30. Benchmark: accurate relative energies obtained at the all-electron CCSDT(Q)/complete-basis-set quality from ref 35.

dx.doi.org/10.1021/jp5028965 | J. Phys. Chem. A 2014, 118, 3243−3252

3. KINETICS COMPUTATIONAL DETAILS

a. VTST/MT Approach. Using the new PES-2014 surface, the reaction path was calculated by starting from the saddle point geometry and going downhill to both reactants and products in mass-weighted Cartesian coordinates, using Page and McIver's method[36] with a step-size of 0.001 $u^{1/2}$ a_0, obtaining the minimum energy path, MEP.[37] The Hessian matrix was evaluated at every point along this reaction path. Along this minimum energy path (MEP), the reaction coordinate, s, is defined as the signed distance from the saddle point, with $s > 0$ referring to the product side. In the rest of paper, the unit of s is a_0, and all calculations are carried out in mass-scaled coordinates with a reduced mass μ equal to 1 u. Thus, distances through the mass-scaled coordinates in a_0 are equivalent to distances through mass-weighted coordinates in $u^{1/2}$ a_0. We calculate the reaction path between $s = -3.0$ and $s = +3.0$ a_0; all rate constants are well converged with respect to the gradient step size, distance between Hessian matrices, and extent of reaction path calculated.

Along the MEP, we calculated the vibrational frequencies after having projected out the motion along the reaction path using curvilinear redundant internal coordinates.[38,39] These coordinates are a nonlinear function of Cartesian coordinates, and they avoid unphysical imaginary values of the vibrational frequencies over a wide range of the reaction coordinate. With this information, we calculated the ground-state vibrationally adiabatic potential curve as

$$V_a^G(s) = V_{MEP}(s) + \varepsilon_{int}^G(s) \tag{3}$$

where s is the reaction coordinate, measured as the mass-weigthed distance along the reaction path to the saddle point, for which $s = 0$, $V_{MEP}(s)$ is the classical energy along the MEP with its energy zero at the reactants, and $\varepsilon_{int}^G(s)$ is the zero-point energy at s.

Rate coefficients were calculated using canonical variational transition-state theory (CVT),[40,41] which locates the dividing surface between reactants and products at a point $s^{*,CVT}(T)$ along the reaction path that minimizes the generalized TST rate coefficients, $k^{GT}(T,s)$ for a given temperature T. Thermodynamically, this is equivalent to locating the transition state at the maximum $\Delta G^{GT,0}[T,s^{*,CVT}(T)]$ of the free energy of activation $\Delta G(T,s)$.[40,41] Thus, the thermal rate coefficient will be given by

$$k^{CVT}(T) = \sigma\frac{k_B T}{h}K^\circ \exp[-\Delta G(T, s^{*,CVT})/k_B T] \tag{4}$$

with k_B being Boltzmann's coefficient, h being Planck's constant, σ being the symmetry factor (the number of equivalent reaction paths, which were assumed to be 4), and K° being the reciprocal of the standard-state concentration, taken as 1 molecule cm^{-3}. The analysis of the $V_a^G(s)$ curve showed the existence of two maxima; therefore, the rate coefficients were finally calculated using the canonical unified statistical model (CUS),[41,42]

$$k^{CUS}(T) = k^{CVT}(T)R^{CUS}(T) \tag{5}$$

with

$$R^{CUS}(T) = \left[1 + \frac{k^{CVT}}{k^{max}} + \frac{k^{CVT}}{k^{min}}\right]^{-1} \tag{6}$$

where k^{CVT} is calculated at the highest maximum of ΔG, k^{max} at the second highest maximum, and k^{min} at the minimum of ΔG, measured from the reactants. $R^{CUS}(T)$ is so a measure of the recrossing effect.

In calculating electronic partition functions, we included the spin−orbit splitting of $O(^3P)$, which is 158.26 and 226.98 cm^{-1} for $^3P_1$ and $^3P_0$ relative to $^3P_2$. We also included the two electronic states for the OH product in the calculation of its electronic partition function, with a 140 cm^{-1} splitting. As a consequence of the electronic degeneracy (Jahn−Teller effect), the potential energy surface for the $O(^3P) + CH_4$ reaction splits into two surfaces of respective symmetries $^3A'$ and $^3A''$. Because our calculations are only based on the lowest surface, the two surfaces, however, making almost equal contributions to the rate, the electronic partition coefficients of the triplet ground-electronic-state generalized transition states are multiplied by 2, yielding an overall value of 6. This is equivalent to using the following total electronic partition function ratio

$$Q_e(T) = \frac{6}{5 + 3e^{-\varepsilon(^3P_1)/RT} + e^{-\varepsilon(^3P_0)/RT}} \tag{7}$$

The rotational partition functions were calculated classically and quantum effects in motions orthogonal to the reaction path were included by using quantum-mechanical vibrational partition functions in the harmonic approximation in redundant internal coordinates.

Finally, we considered the tunneling contributions. This reaction has a heavy−light−heavy mass combination, and therefore, a large curvature tunneling (LCT) calculation should be considered.[43] We also considered the microcanonical optimized multidimensional tunneling (μOMT) approach[44] in which, at each total energy, the larger of the small-curvature (SCT)[45] and large-curvature (LCT) tunneling probabilities is taken as the best estimate. In the LCT approximation, tunneling proceeds along straight-line paths from the entrance valley of the PES to the product valley and perpendicular to the reaction path, and two versions of this method, LCT3[41] and LCT4,[46] have been developed. A better way to compute tunneling is to optimize the angle between the reaction path and the tunneling path so that the tunneling probability is the highest or the imaginary action is the least. This angle is 0° in the SCT case and 90° in the LCT case. This is (very briefly described) the least-action tunneling (LAT).[47] The LAT method is considered to be the most accurate, but it has not been developed for polyatomic reactions until very recently,[48] and it has been scarcely applied.

All kinetics calculations were performed using the POLYRATE-2010 code developed by Truhlar and co-workers.[49]

b. RPMD Approach. Ring polymer molecular dynamics (RPMD) is a recently proposed full-dimensional approach to treat quantum real-time dynamics of the system on the basis of the classical isomorphism between the quantum system and classical ring polymer consisting of n copies (beads) of this system interacting through harmonic interaction.[34] This isomorphism allows us to approximate the quantum real-time dynamics using the classical real-time evolution in an extended phase space of the ring polymer. The RPMD rate coefficient is rigorously independent of the choice of the transition state dividing surface used to compute it, a feature that distinguishes it from all transition-state-theory-based methods.[34]

Application of RPMD to gas-phase bimolecular chemical reactions[50−59] has demonstrated that it provides systematic and consistent performance across a wide range of system

dx.doi.org/10.1021/jp5028965 | J. Phys. Chem. A 2014, 118, 3243−3252

dimensionalities. In all systems considered so far, the RPMD rate coefficient captures almost perfectly the ZPE effect and is usually within a factor of 2−3 of accurate results at very low temperatures in the deep quantum tunneling regime when compared to rigorous quantum mechanical results available for these systems. Most chemical reactions can be studied using RPMD with only about 1−2 order(s) of magnitude higher computational costs than conventional quasi-classical trajectory (QCT) calculations.

The RPMD calculations were carried out using the RPMDrate code developed by Suleimanov and co-workers;[50] the working equations of the RPMD rate theory can be found in refs 34 and 50. The input parameters are summarized in Table 1. We also repeated our calculations at 2500 K with one ring polymer bead, which corresponds to purely classical simulation.[34] Note that as in the VTST case all rate coefficients are corrected with the electronic partition function given by eq 7.

Table 1. Input Parameters for the RPMDrate Calculations on the O + CH_4 Reaction[a]

parameter	O + CH_4	explanation
	Command Line Parameters	
temp	200−2500	temp (K)
N_{beads}	128−4	no. of beads (RPMD calculations)
	1	no. of beads (classical calculations at 2500 K)
	Dividing Surface Parameters	
R_∞	15	dividing surface s_1 parameter (a_0)
N_{bonds}	1	number of forming and breaking bonds
$N_{channel}$	4	number of equivalent product channels
	Thermostat	
thermostat	"Andersen"	thermostat option
	Biased Sampling Parameters	
$N_{windows}$	111	no. of windows
ξ_1	−0.05	center of the first window
$d\xi$	0.01	window spacing step
ξ_N	1.05	center of the last window
dt	0.0001	time step (ps)
k_i	2.72	umbrella force constant ((T/K) eV)
$N_{trajectory}$	200	no. of trajectories
$t_{equilibration}$	20	equilibration period (ps)
$t_{sampling}$	100	sampling period in each trajectory (ps)
N_i	2×10^8	total no. of sampling points
	Potential of Mean Force Calculation	
ξ_0	−0.02	start of umbrella integration
$\xi^\#$	1.05	end of umbrella integration[b]
N_{bins}	5000	no. of bins
	Recrossing Factor Calculation	
dt	0.0001	time step (ps)
$t_{equilibration}$	20	equilibration period (ps) in the constrained (parent) trajectory
$N_{total\ child}$	100 000	total no. of unconstrained (child) trajectories
$t_{child\ sampling}$	20	sampling increment along the parent trajectory (ps)
N_{child}	100	no. of child trajectories per one initially constrained configuration
t_{child}	0.1	length of child trajectories (ps)

[a]The format of the input file is explained in detail in the RPMDrate code manual (see ref 50 and http://www.mit.edu/~ysuleyma/rpmdrate). [b]Maximum value of the free energy is detected automatically by RPMDrate.

4. RESULTS AND DISCUSSION

Table 2 lists the theoretical forward rate coefficients in the temperature range 200−2500 K obtained with the PES-2014 surface, together with experimental rate coefficients[18,21] for comparison. Figure 2 shows the corresponding Arrhenius plots.

Table 2. Thermal Rate Coefficients for the $O(^3P)$ + CH_4 Reaction[a]

	theoretical		experimental	
T (K)	CUS/LAT	RPMD	ref 18	ref 21
200	1.94×10^{-19}	1.29×10^{-19}		
300	1.32×10^{-17}	1.50×10^{-17}	9.00×10^{-18}	5.50×10^{-18}
400	2.28×10^{-16}	3.17×10^{-16}	3.40×10^{-16}	3.00×10^{-16}
500	1.84×10^{-15}	2.37×10^{-15}		3.65×10^{-15}
600	8.95×10^{-15}	1.30×10^{-14}	1.70×10^{-14}	2.00×10^{-14}
1000	3.60×10^{-13}	5.41×10^{-13}	6.00×10^{-13}	7.70×10^{-13}
1500	2.95×10^{-12}	4.58×10^{-12}	5.00×10^{-12}	6.00×10^{-12}
2000	1.03×10^{-11}	1.90×10^{-11}	1.80×10^{-11}	1.90×10^{-11}
2500	2.37×10^{-11}	4.05×10^{-11}	4.20×10^{-11}	4.20×10^{-11}

[a]In cm^3 $molecule^{-1}$ s^{-1}.

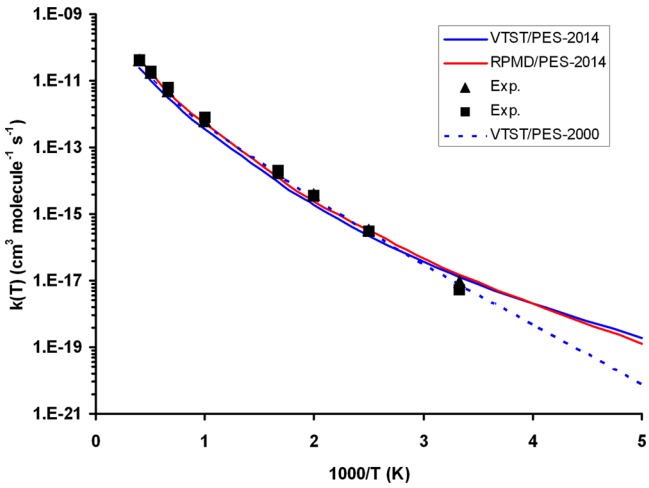

Figure 2. Arrhenius plots of the $O(^3P)$ + CH_4 rate coefficients computed using the PES-2014 surface: CUS/LAT, solid blue line; RPMD, solid red line; exp from ref 18, solid squares; exp from ref 21, solid triangles; CUS/LCT-3 using PES-2000 from ref 24, dashed blue line.

Except for the lowest temperature (200 K), the RPMD rate coefficients are larger than the CUS/LAT and the difference increases with temperature. At 2500 K, the RPMD rate coefficient is higher than the CUS/LAT counterpart by a factor of almost 2. Because RPMD rate theory is exact in the classical high-temperature limit,[34] these results suggest that the CUS/LAT method underestimates the rate coefficients, and this is possibly related to approximations used in the TST-based methods.[59,60] This point is also confirmed by excellent agreement of the RPMD rate coefficients with experimental values at 400−2500 K.

To deeply analyze the reason behind this discrepancy between CUS/LAT and RPMD at high temperatures, we performed additional calculations at 2500 K using conventional TST (i.e., locating the transition state dividing surface at the saddle point), CVT, and CUS implemented in POLYRATE-2010. In both cases tunneling is included by means of the LAT

dx.doi.org/10.1021/jp5028965 | J. Phys. Chem. A 2014, 118, 3243−3252

method, although it is expected to be negligible at such a high temperature. TST and CVT differ in the location of the transition state, but CVT considers that only the variational TST bottleneck controls the rate coefficient. CUS, however, takes into account other relative maxima on the free energy curve and the possibility that the system can be thermalized in one of the minima between two maxima. Thus, the CVT recrossing factor, computed as the ratio between CVT and TST rate coefficients, measures the effect of the displacement of the maxima of the free energy curve from the saddle point, also known as "variational effect", whereas the CUS recrossing factor (CUS rate coefficient over TST rate coefficient) additionally includes the effect of the multiple maxima on recrossing.

We compare these rate coefficients with the RPMD, pure classical TST, and classical TST (locating the dividing surface at the saddle point) counterparts obtained using RPMDrate in Table 3. The classical results by RPMDrate were obtained by

Table 3. Thermal Rate Coefficients for the $O(^3P) + CH_4$ Reaction at 2500 K Using Different Dynamical Methods (Description in Text)

method	$k(T=2500\ K)$, $cm^3\ molecule^{-1}\ s^{-1}$
POLYRATE	
CUS/LAT	2.37×10^{-11}
CUS	2.29×10^{-11}
CVT/LAT	2.55×10^{-11}
CVT	2.46×10^{-11}
classical TST with quantum vibrational partition functions (harmonic approximation)[a]	7.05×10^{-11}
classical TST with classical vibrational partition functions (harmonic approximation)[a]	6.11×10^{-11}
RPMDrate	
RPMD	4.05×10^{-11}
classical	3.54×10^{-11}
classical TST[a]	7.94×10^{-11}

[a]Obtained by placing the dividing surface at the saddle point.

setting the number of ring polymer beads to one.[34] We first note that at the highest temperature considered in this work, 2500 K, the difference between pure classical and RPMD rate coefficient is only 15%, which shows that we achieved the classical high-temperature limit where all quantum mechanical effects become practically negligible. The POLYRATE results confirm this point: the difference between TST calculations with classical and quantum partition functions is also within 15%. The LAT correction for tunneling is 1.036 and is negligible, as expected at such high temperature. However, a noticeable discrepancy is observed between the classical TST rate coefficients obtained using these two codes. The classical TST rate coefficient obtained by RPMDrate using full-dimensional classical molecular dynamics is 30% higher than the one obtained using partition functions evaluated with POLYRATE. The difference between these two rate coefficients can only be attributed to effects of anharmonicity, mode−mode coupling, or the approximation of considering the reaction coordinate motion as separable.

From Table 3 we can infer that the CVT and CUS rate coefficients are almost the same, and the recrossing factor, CUS/TST = 0.3248, is almost exclusively due to the variational shift of the maximum of the free energy curve from the saddle point (at 2500 K the transition state is located at $s = -0.315\ a_0$ in the entrance channel). In the previous study by one of us[61] the importance of the anharmonicity on the final rate constants was analyzed in detail for the benchmark $Cl + H_2$ reaction. It was found that, when the lowest modes are treated as anharmonic oscillators, the motion along the reaction coordinate leads to a larger decrease of the zero-point energy than when the harmonic approach is used. When the lowest vibrational modes are treated using harmonic approximation, this leads to overprediction of their contribution shifting the free energy maximum from the saddle point and thus overestimating the variational effects.

In the case of the title polyatomic reaction, the anharmonic calculation is not so straightforward, because anharmonicity is not included for curvilinear coordinates or large-curvature tunneling methods in the POLYRATE-2010 code.[49] It is only implemented using the rectilinear coordinates, which exhibit unphysical imaginary values of the vibrational frequencies for the present system. However, to put into in evidence this effect at least qualitatively, we have calculated anharmonicity of the stretching modes using the Wentzel−Kramers−Brillouin (WKB) approximation,[62] taking into account the following considerations about the calculation in nonstationary points (i.e., points along the reaction path) and about the proper WKB method.

Computing anharmonic vibrations only on the stationary points will not shed any light on the subject, because we are proposing that the main effect of anharmonicity is that it would reduce variational effects, thus increasing the rate constants. Therefore, we need to compute variational TST rate constants using anharmonic vibrations to see if our assumption is correct. Unfortunately, performing an accurate anharmonic vibrational analysis on nonstationary points is far from being straightforward. On nonstationary points we need to project out from the Hessian matrix the motion in the direction of the reaction path, which is obtained from the gradient. One needs an accurate gradient and Hessian calculation to obtain meaningful results because numerical errors can change the direction that is projected out. Additionally, numerical errors get amplified when third- or even fourth-order derivatives are computed. On top of it all, some vibrations become so floppy along the reaction path that numerical errors can be bigger than the effect of the vibration itself. Numerical errors enter in an exponential way on the partition functions, causing significant noise on the free energy curve, and rate constants are exponential functions of this free energy. Bumpy free energy curves produce unaccurate rate constants. Therefore, one has to be extremely cautious and try to remove all significant numerical errors in the calculation.

But numerical problems are not the only issue. To the best of our knowledge, no general method has been proposed to successfully deal with anharmonicity for polyatomic systems along a reaction path. For example, Isaacson[63,64] developed a method using perturbation theory that seems to be promising. However, it has only been applied to three- or four-atom reactions. Moreover, perturbation theory for degenerate vibrations can be problematic due to the presence of Fermi resonances. Thus, when we tried to apply perturbation theory to our calculations using standard codes, we did not get physically meaningful results.

Finally, we evaluated the ground-state vibrational energies by using the WKB approximation as implemented in POLYRATE-2010. This method is designed for stretching modes, and we believe that the most anharmonic vibration is the symmetric

dx.doi.org/10.1021/jp5028965 | J. Phys. Chem. A 2014, 118, 3243−3252

stretch of the C−H−O system, which we sometimes call the reactive mode because it is the mode more related to the hydrogen transfer. However, in its present implementation this approach is used only for the vibrational ground state whereas higher energy vibrational levels (used in the calculation of the partition functions) are obtained by harmonic approximations. Therefore, our approach to the problem is only qualitative. Figure 3 shows the vibrationally adiabatic ground-state curve

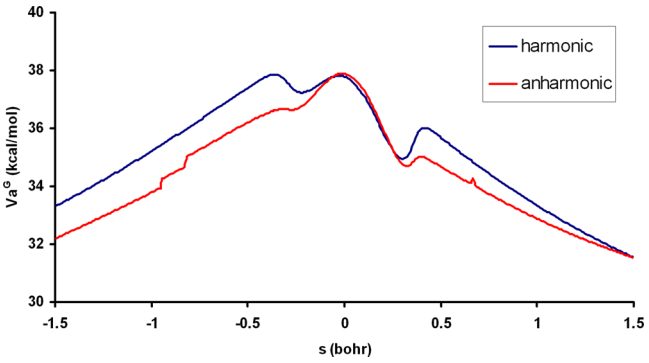

Figure 3. Vibrationally adiabatic ground-state potential energy, $V_a^G(s)$. The blue line is based on harmonic zero-point energies, and the red line is based on anharmonic zero-point energies.

(V_a^G) near the top of the barrier, where motions are less floppy and the anharmonic methods work best. The blue line is computed using harmonic vibrations, whereas the red line is computed using the anharmonic results. The sudden increase in the vibration of the reactive mode causes the peak to the left of the saddle point. The presence of this peak shifts the transition state from the saddle point to a point around $s = -0.3$ bohr at 2000 K and is much softened when the vibrational energy is computed with the WKB method. Therefore, one would expect that, according to our previous discussion, the harmonic approximations overestimate the importance of variational effects, and under an anharmonic approximation one would expect higher rate constants at those temperatures where variational effects are more significant, i.e., at the higher temperature range.

Reverting back to Table 2, let us analyze now the low temperatures regime ($T \leq 300$ K). Both CUS and RPMD methods overestimate the experimental rate coefficients, although this comparison must be taken with caution due to the experimental difficulties in the deep tunneling regime. From the previous studies,[34,50−58] one can expect that RPMD method will overestimate the exact quantum mechanical (QM) rates for an asymmetric reaction by about a factor of no more than 2−3 at low temperatures. At the same time, for the title reaction on the PES-2000, the RPMD demonstrated perfect agreement with the rigorous quantum mechanical calculations though, as discussed in Introduction, the previous PES-2000 should exhibit less tunneling.[51] We suggest that rigorous quantum mechanical calculations on PES-2014 will be of invaluable help in solving this puzzle. We also suggest that the LAT method overestimates tunneling for the title reaction at the lowest temperatures considered, e.g., at 200 K where it gives higher values than RPMD. In fact, when the LCT-4 version is used, a better agreement with experiment at 300 K is obtained, 1.0×10^{-17} cm^3 molecule^{-1} s^{-1}, whereas the LCT-3 version overestimates this effect, giving a poor agreement with experiment, 4.4×10^{-17} cm^3 molecule^{-1} s^{-1}. However, it is worth noting that both RPMD and CUS/LAT results show a similar behavior of the curvature of the Arrhenius plot, which is more pronounced than the $k(T)$ recommended in the literature (eq 2) due to a large tunneling contribution at low temperatures (Figure 2).

As was noted before, the influence of the semiclassical approaches to estimate tunneling in the VTST method is very important and it deserves further analysis. For the title reaction at the lowest temperature analyzed, 200 K, LCT-3 gives the higher tunneling coefficient, $\kappa = 7310.0$, whereas the LCT-4 version gives the lower coefficient, $\kappa = 929.4$, with the LAT approach in an intermediate situation, $\kappa = 2569.0$. The imaginary action integrals are plotted in Figure 4 (upper

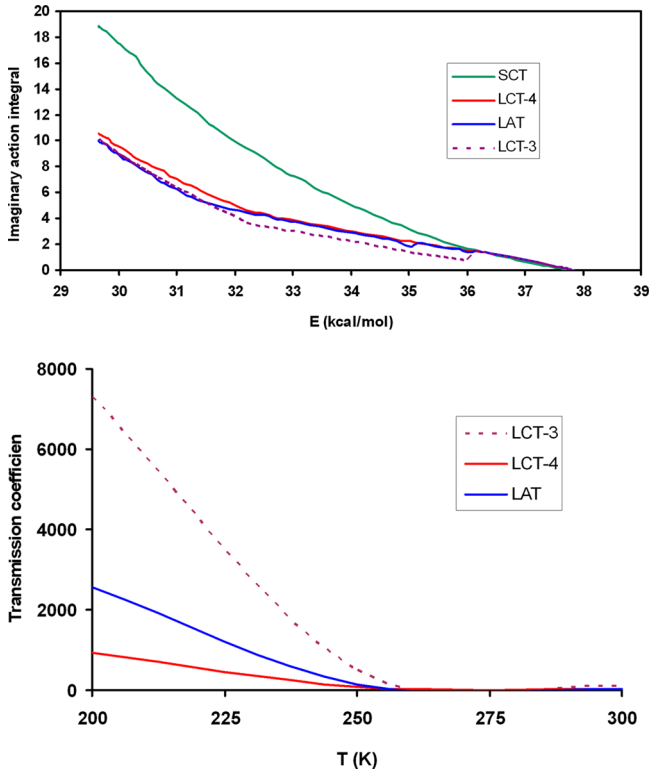

Figure 4. Upper panel: Imaginary action integral computed using the SCT method (green line), LCT version 4 (red line), LAT method (blue line), and LCT version 3 (dashed line) methods as a function of the energy. The zero of energy is set to reactants' potential energy. Lower panel: transmission coefficients computed using LCT version 3 (dashed line), LCT version 4 (red line), and LAT (blue line).

panel). The SCT approach gives, obviously, the highest values, related to the lowest tunneling contributions, as was expected in this heavy−light−heavy mass combination. The LAT and LCT-4 present similar behavior in all energy ranges, which is also expected because LAT is based on the LCT-4 probabilities. The closeness between these two methods clearly indicates that variational optimization of the tunneling path has a relatively minor effect and that the reaction is a large-curvature tunneling reaction. The LCT-3 approach gives the lowest values of the action integral and consequently the largest transmission factors. As noted elsewhere,[44] this is due to the total neglect of the anharmonicity of the motions orthogonal to the reaction path. These effects are also clearly observed in the same Figure 4 (lower panel), where the transmission factor is plotted against temperature. The LCT-3 approach overestimates the tunneling

dx.doi.org/10.1021/jp5028965 | J. Phys. Chem. A 2014, 118, 3243−3252

contribution, whereas the LCT4 and LAT approaches, which deal in a better way with the anharmonicity of the modes orthogonal to the tunneling path, give more reasonable values. In sum, we suggest that both CUS/LAT and RPMD overestimate the tunneling contribution, although the first one is in larger extension in the deep-tunneling regime (200 K). Therefore, we note that further accurate quantum mechanical calculations based on the PES-2014 are required to assess rigorously the tunneling factor for the present system.

In Figure 2 we also include the results obtained with the PES-2000 surface for comparison. At low temperatures (T < 300 K) it presents less tunneling than the PES-2014 surface, which is the expected behavior because the barrier is broader, whereas at higher temperatures (T > 300 K) it reproduces the experimental data, which is not surprising because, as was noted in the Introduction, the PES-2000 surface is semiempirical; i.e., the experimental rate coefficients were used in the fitting process.

Table 4 lists the phenomenological activation energies computed as local slopes of Arrhenius plots, to provide the most appropriate comparison with experiment. Both theoretical results, RPMD and CUS/LAT, increase with temperature, reproducing the experimental evidence. However, the behavior at low and high temperatures is very different. At low temperatures, the theoretical values underestimate the experiment but at high temperatures the agreement is better. We stress on the fact that both the intrinsic experimental difficulties and the limitations of semiclassical methods in the deep tunneling regime can be responsible for the observed discrepancy between theory and experiment.

Table 4. Theoretical and Experimental Activation Energies (kcal mol^{-1})

	temperature, K				
method	300−400	400−500	500−600	900−1500	1500−2500
CUS/LAT	6.8	8.3	9.4	12.5	15.5
RPMD	7.3	8.0	10.2	11.4	16.2
exp[a]	8.7	9.1	10.1	12.4	15.8
exp[b]	9.6	9.9	10.5	12.0	14.4

[a]Reference 18. [b]References 13 and 21.

The activation energies at 298 K (from slopes of Arrhenius plots from 293 to 303 K) are 5.98 and 3.17 kcal mol^{-1} for the forward and reverse reactions from the CUS/LAT method, respectively. Using these theoretical activation energies, a value of 2.81 kcal mol^{-1} is obtained for the enthalpy of reaction at 298 K, in agreement with the experimental value from enthalpies of formation, ΔH_r(298 K) = 2.85 kcal mol^{-1} (ref 65). This result confirms some overall characteristics of the analytical surface, and the balance of the forward and reverse reactions.

We have also analyzed the deuterated analogue, O(^{3}P) + CD_4 (Figure 5). In contrast with the O(^{3}P) + CH_4 reaction, note first that the free energy curve for the deuterated analogue presents a maximum located very close to the saddle point. Therefore, the "variational" and recrossing effects (important at high temperatures) are practically negligible in this case. Second, due to transfer of the heavier deuterium atom, less tunneling (important at low temperatures) is present. As it was expected, now the agreement between RPMD and CUS/LAT is better, with an average difference smaller than 10% in the common temperature range (see Arrhenius plot in Figure 5).

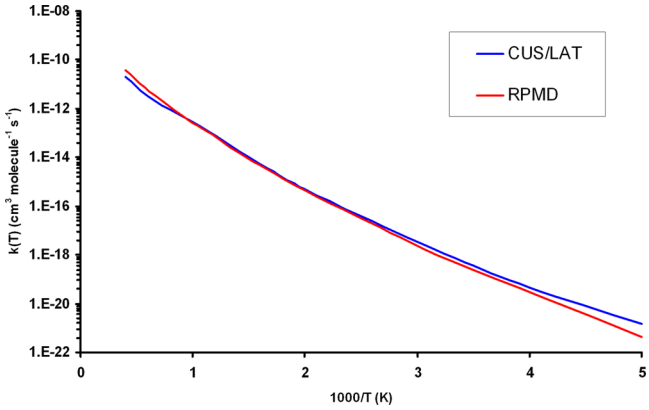

Figure 5. Arrhenius plots of the O(^{3}P) + CD_4 rate coefficients computed using the PES-2014 surface: CUS/LAT, solid blue line; RPMD, solid red line.

However, at high temperatures (2500 K) the agreement is reasonable but at low temperatures (200 K) the agreement is very poor, with a RPMD/CUS-LAT factor of 0.31 demonstrating the important discrepancy in treating the tunneling effect. As indicated above, further rigorous quantum mechanical calculations for the title reaction are necessary for assessing accuracy of these two approaches at low temperatures.

To complete the kinetic study, we calculated the kinetics isotope effects (KIEs) (defined as the ratio of the rate coefficients of the unsubstituted reaction to the deuterated reaction, CH_4/CD_4). As a ratio of rate coefficients, the KIEs are less sensitive to the accuracy of the PES, representing an excellent opportunity to test the dynamics approaches. As far as we know, no experimentally determined isotope data are available for comparison and we hope that the present study will stimulate experiment.

The calculated KIEs from this work and the previous ones[24] using the PES-2000 surface are listed in Table 5. In the whole temperature range (200−2500 K) the ratio between RPMD and CUS/LAT KIEs vary by factors between 2.1 and 1.0, decreasing with temperature; i.e., the reactive system approaches the classical behavior, where the recrossing and quantum effects are negligible. At the highest temperatures (T ≥ 1500 K) both methods agree with each other. Because RPMD is exact in the high temperature regime, these results suggest that the harmonic approximation implemented in the

Table 5. H/D Kinetic Isotope Effects for the O(^{3}P) + CH_4 /CD_4 Reactions

	PES-2014		PES-2000
T (K)	RPMD	VTST[a]	VTST[b]
200	290.4	136.6	64.8
300	30.8	18.6	18.9
400	10.7	6.2	8.4
500	5.1	3.4	3.4
600	3.8	2.4	2.2
1000	2.0	1.43	1.4
1500	1.3	1.40	0.98
2000	1.3	1.25	0.82
2500	1.1	1.10	0.93

[a]Calculated using the CUS/LAT level. This work. [b]Calculated using the CUS/LCT-3 level, from ref 24.

dx.doi.org/10.1021/jp5028965 | J. Phys. Chem. A 2014, 118, 3243−3252

CUS/LAT calculations leads to underestimation of the rate coefficients but cancels out in the KIE. The systematic and consistent performance of RPMD rate theory usually contrasts with the performance of TST-based methods, which can both overestimate and underestimate KIEs.[34,55] At low temperatures, where tunneling is important, in similar hydrogen abstraction reactions with heavy−light−heavy mass combination, OH + CH_4, Suleimanov and co-workers[55] found that the RPMD approach overestimates the KIEs, and concluded that because the deuterated reaction presents less tunneling, the RPMD rate coefficients will be more accurate than the corresponding nondeuterated reaction. As a result, the overestimation of the KIE at low temperatures is due to the overprediction of the rate coefficients for the nondeuterated asymmetric reaction. At the same time, we also note that RPMD provided quantitative agreement for the title (nondeuterated) reaction even at very low temperatures on PES-2000.[51] Therefore, for the present reaction, these results suggest that experimental KIEs should be close or no more than 2−3 times lower that the RPMD counterparts at very low temperatures.

In sum, when one compares theory and experiment many factors must be taken into account: experimentally, the quality and accuracy of the measures and, theoretically, the dynamics methods used and the accuracy of the PES. So, in a comparison theory/experiment, both the dynamics method and the PES are tested, whereas in a theoretical comparison using the same PES, the approaches and limitations in the dynamics methods are being tested.

5. CONCLUSIONS

In this work we have investigated the kinetics of the gas-phase reaction $O(^3P)$ + CH_4 → OH + CH_3 and its deuterated analogue, using two dynamical approaches−ring polymer molecular dynamics (RPMD) and variational transition-state theory with canonical unified statistical model and transmission coefficients calculated by the least-action tunneling approximation (CUS/LAT), based on new analytical full-dimensional potential energy surface (PES), PES-2014.[30] We found that, when the oxygen atom approaches CH_4, the reaction evolves with a high and thin barrier, which favors the tunneling, with stabilized intermediate complexes in the entrance and exit channels.

In the low temperature regime, both approaches present noticeable curvature in the Arrhenius plots, indicating the important role played by tunneling. This curvature is more pronounced than experimentally reported. Because the experimental measurements in this regime are problematic, we believe that these results can encourage to experimentalists to study more deeply the low-temperature kinetics.

In the classical high-temperature limit regime, where the RPMD rate theory is exact,[34] this approach agrees with experiment perfectly, indicating the VTST/MT underestimates the rate coefficients by almost a factor of 2. Although further work would be required to explain this behavior, we believe that the reason is related to the harmonic separable-modes approximation used for computing the partition functions in the CUS/LAT method. One would expect that anharmonicity plays a more significant role at high temperatures, where higher vibrational levels are more populated. On the other hand, very good agreement between RPMD and experiment at high temperatures, indirectly lends confidence in the accuracy of the PES-2014.

The kinetic isotope effect (KIE) is another very sensitive test of dynamical approaches. The CUS/LAT and RPMD exhibit reasonable agreement in the high-temperature range but at low temperatures the RPMD KIEs are larger. Because no experimental results are available to shed any light in this comparison, we think that experimentalists may be encouraged to study more deeply the kinetics of this reaction, although we are aware of the very great experimental difficulty involved, especially at low temperatures.

AUTHOR INFORMATION

Corresponding Authors

*Y. V. Suleimanov: e-mail, ysuleyma@mit.edu.

*J. Espinosa-Garcia: e-mail, joaquin@unex.es.

Notes

The authors declare no competing financial interest.

ACKNOWLEDGMENTS

This work was partially supported by Gobierno de Extremadura, Spain, and FEDER (Project No. IB10001). Y.V.S. and W.H.G. acknowledge the support of the Combustion Energy Frontier Research Center, an Energy Frontier Research Center funded by the U.S. Department of Energy, Office of Basic Energy Sciences under Award Number DE-SC0001198.

REFERENCES

(1) Cadle, R. D.; Allen, E. R. Kinetics of the Reaction of $O(^3P)$ with Methane in Oxygen, Nitrogen, and Argon-Oxygen Mixtures. *J. Phys. Chem.* **1965**, *69*, 1611−1615.

(2) Brown, J. M.; Trush, B. A. ESR Studies of the Reactions of Atomic Oxygen and Hydrogen with Simple Hydrocarbons. *Trans. Faraday Soc.* **1967**, *63*, 630−642.

(3) Wong, E. L.; Porter, A. E. Mass-spectrometric Investigation of Reaction of Oxygen Atoms with Methane. *Can. J. Chem.* **1967**, *45*, 367−371.

(4) Froben, F. W. Die Reaktion von 0-Atomen mit Methan, Chloroform und Tetrachlorkohlenstoff. *Ber. Bunsen-Ges. Phys. Chem.* **1968**, *72*, 996−998.

(5) Westenberg, A. A.; DeHaas, N. Reinvestigation of the Rate Coefficients for O+H_2 and O+CH_4. *J. Chem. Phys.* **1969**, *50*, 2512−2516.

(6) Herron, J. T. An Evaluation of Rate Data for the Reactions of Atomic Oxygen (O^3P) with Methane and Ethane. *Int. J. Chem. Kinet.* **1969**, *1*, 527−539.

(7) Dean, A. M.; Kistiakowsky, G. B. Oxidation of Carbon Monoxide/Methane Mixtures in Shock Waves. *J. Chem. Phys.* **1971**, *54*, 1718−1725.

(8) Herron, J. T.; Huie, R. E. Rate Constants for the Reactions of Atomic Oxygen (O ^3P) with Organic Compounds in the Gas Phase. *J. Phys. Chem. Ref. Data* **1973**, *2*, 467−518.

(9) Barassin, J.; Combourieu, J. Etude Cinetique des Reactions entre l'Oxygene Atomique et les Derives Chlores du Methane. II. Reactions CH_3Cl + O, $CHCl_3$ + O, CCl_4 + O et CH_4 + O: Resultats Experimentaux. *J. Bull. Soc. Chim. Fr.* **1974**, *1*, 1−6.

(10) Brabbs, T. A.; Brokaw, R. S. Shock Tube Measurements of Specific Reaction Rates in the Branched Chain CH_4−CO−O_2 System. *15th Symp. (Int.) Combust.* **1975**, 893−901.

(11) Roth, P.; Just, Th. Atomabsorptionsmessungen zur Kinetik der Reaktion CH_4 + O → CH_3 + OH im Temperaturbereich 1500 ≤ T ≤ 2250 K. *Ber. Bunsen-Ges. Phys. Chem.* **1977**, *81*, 572−577.

(12) Shaw, R. Semi-empirical Extrapolation and Estimation of Rate Constants for Abstraction of H from Methane by H, O, HO, and O_2. *J. Phys. Chem. Ref. Data* **1978**, *7*, 1179−1190.

(13) Klemm, R. B.; Tanzawa, T.; Skolnik, E. G.; Michael, J. V. A Resonance Fluorescence Kinetic Study of the $O(^3P)$+CH_4 Reaction

over the Temperature Range 474 to 1156 K. *18th Symp. (Int.) Combust.* **1981**, 785−799.
(14) Fontijn, A.; Kurzius, S. C.; Houghton, J. J. High-temperature Fast-flow Reactor Studies of Metal-atom Oxidation Kinetics. *14th Symp. (Int.) Combust.* **1973**, 167−174.
(15) Warnatz, J. Rate Coefficients in the C/H/O systems. In *Combustion Chemistry*; Gardner, W. C., Ed.; Springer-Verlag: New York, 1984; Chapter 5.
(16) Sutherland, J. W.; Michael, J. V.; Klemm, R. B. Rate Constant for the $O(^3P) + CH_4 = OH + CH_3$ Reaction Obtained by the Flash Photolysis-shock Tube Technique over the Temperature Range 760 < T < 1760 K. *J. Phys. Chem.* **1986**, *90*, 5941−5945.
(17) Wagner, A. F.; Dunning, T. H.; Walch, S. P.; Schatz, G. S. Reported in ref 21.
(18) Cohen, N. A Reevaluation of Low Temperature Experimental Rate Data for the Reactions of O Atoms with Methane, Ethane, and Neopentane. *Int. J. Chem. Kinet.* **1986**, *18*, 59−82.
(19) Tsang, W.; Hampson, R. F. Chemical Kinetic Data Base for Combustion Chemistry. Part I. Methane and Related Compounds. *J. Phys. Chem. Ref. Data* **1986**, *15*, 1087−1290.
(20) Herron, J. T. Evaluated Chemical Kinetic Data for the Reactions of Atomic Oxygen $O(^3P)$ with Saturated Organic Compounds in the Gas Phase. *J. Phys. Chem. Ref. Data* **1988**, *17*, 967−1026.
(21) Baulch, D. L.; Cobos, C. J.; Cox, R. A.; Esser, C.; Frank, P.; Just, Th.; Kerr, J. A.; Pilling, M. J.; Troe, J.; Walker, R. W.; Warnatz, J. Evaluated Kinetic Data for Combustion Modelling. *J. Phys. Chem. Ref. Data* **1992**, *21*, 411−752.
(22) Corchado, J. C.; Espinosa-Garcia, J.; Neto, O. R.; Chiang, Y. Y.; Truhlar, D. G. Dual-Level Direct Dynamics Calculations of the Reaction Rates for a Jahn-Teller Reaction: Hydrogen Abstraction from CH_4 or CD_4 by $O(^3P)$. *J. Phys. Chem. A* **1998**, *102*, 4899−4910.
(23) Clary, D. C. Quantum Dynamics of the $O(^3P)+CH_4 \rightarrow CH_3+OH$ Reaction. *Phys. Chem. Chem. Phys.* **1999**, *1*, 1173−1179.
(24) Espinosa-Garcia, J.; García-Bernaldez, J. C. Analytical Potential Energy Surface for the $CH_4 + O(^3P) = CH_3 + OH$ Reaction. Thermal Rate Constants and Kinetic Isotope Effects. *Phys. Chem. Chem. Phys.* **2000**, *2*, 2345−2351.
(25) Huarte-Larrañaga, F.; Manthe, U. Accurate Quantum Dynamics of a Combustion Reaction: Thermal Rate Constants of $O(^3P)+CH_4(X^1A_1) \rightarrow OH(X^2\Pi)+CH_3(X^2A'_2)$. *J. Chem. Phys.* **2002**, *117*, 4635−4638.
(26) Troya, D.; García-Molina, E. Quasiclassical Trajectory Study of the $O(^3P) + CH_4 \rightarrow OH + CH_3$ Reaction with a Specific Reaction Parameters Semiempirical Hamiltonian. *J. Phys. Chem. A* **2005**, *109*, 3015−3023.
(27) Yu, H.-G.; Nyman, G. Quantum Dynamics of the $O(^3P)+CH_4 \rightarrow OH+CH_3$ Reaction: An Application of the Rotating Bond Umbrella Model and Spectral Transform Subspace Iteration. *J. Chem. Phys.* **2000**, *112*, 238−247.
(28) Yang, M.; Lee, S.-Y.; Zhang, D. H. Seven-dimensional Quantum Dynamics Study of the $O(^3P)+CH_4$ Reaction. *J. Chem. Phys.* **2007**, *126*, 064303.
(29) Li, Y.; Suleimanov, Y. V.; Yang, M.; Green, W. H.; Guo, H. Ring Polymer Molecular Dynamics Calculations of Thermal Rate Constants for the $O(^3P) + CH_4 \rightarrow OH + CH_3$ Reaction: Contributions of Quantum Effects. *J. Phys. Chem. Lett.* **2013**, *4*, 48−52.
(30) Gonzalez-Lavado, E.; Corchado, J. C.; Espinosa-Garcia, J. The Hydrogen Abstraction Reaction $O(^3P) + CH_4$. A New Analyical Potential Energy Surface Based on Fit to Ab initio Calculations. *J. Chem. Phys.* **2014**, *140*, 064310.
(31) Walch, S. P.; Dunning, T. H. Calculated Barrier to Hydrogen Atom Abstraction from CH_4 by $O(^3P)$. *J. Chem. Phys.* **1980**, *72*, 3221−3227.
(32) Gonzalez, C.; McDouall, J. J. W.; Schlegel, H. B. Ab initio Study of the Reactions Between Methane and Hydroxyl, Hydrogen Atom, and Triplet Oxygen Atom. *J. Phys. Chem.* **1990**, *94*, 7467−7471.
(33) Richardson, J. O.; Althorpe, S. C. Ring-Polymer Molecular Dynamics Rate-Theory in the Deep-Tunneling Regime: Connection with Semi-Classical Instanton Theory. *J. Chem. Phys.* **2009**, *131*, 214106.
(34) Suleimanov, Y. V.; Collepardo-Guevara, R.; Manolopoulos, D. E. Bimolecular Reaction Rates from Ring Polymer Molecular Dynamics: Application to $H + CH_4 \rightarrow H_2 + CH_3$. *J. Chem. Phys.* **2011**, *134*, 044131.
(35) Czako, G.; Bowman, J. M. Dynamics of the $O+ CH_3D$ Reactions on an Accurate Ab initio Potential Energy Surface. *Proc. Natl. Acad. Sci. U. S. A.* **2012**, *109*, 7997−8001.
(36) Page, M.; McIver, J. W. On Evaluating the Reaction Path Hamiltonian. *J. Chem. Phys.* **1988**, *88*, 922−935.
(37) Fast, P. L.; Truhlar, D. G. Variational Reaction Path Algorithm. *J. Chem. Phys.* **1998**, *109*, 3721−3729.
(38) Jackels, C. F.; Gu, Z.; Truhlar, D. G. Reaction-Path Potential and Vibrational Frequencies in Terms of Curvilinear Internal Coordinates. *J. Chem. Phys.* **1995**, *102*, 3188−3201.
(39) Chuang, Y.-Y.; Truhlar, D. G. Reaction-Path Dynamics in Redundant Internal Coordinates. *J. Phys. Chem. A* **1998**, *102*, 242−247.
(40) Garrett, B. C.; Truhlar, D. G. Generalized Transition State Theory. Bond Energy-Bond Order Method for Canonical Variational Calculations with Applications to Hydrogen Atom Transfer Reactions. *J. Am. Chem. Soc.* **1979**, *101*, 4534−4548.
(41) Truhlar, D. G.; Isaacson, A. D.; Garrett, B. C. Generalized Transition State Theory. In *Theory of Chemical Reaction Dynamics*; Baer, M., Ed.; CRC Press: Boca Raton, FL, 1985; Vol. 4, pp 65−137.
(42) Garret, B. C.; Truhlar, D. G. Canonical Unified Statistical Model. Classical Mechanical Theory and Applications to Collinear Reactions. *J. Chem. Phys.* **1982**, *76*, 1853−1858.
(43) Truong, T. N.; Lu, D.-H.; Lynch, G. C.; Liu, Y. P.; Melissas, V. S.; Stewart, J. J.; Steckler, R.; Garrett, B. C.; Isaacson, A. D.; Gonzalez-Lafont, A.; et al. MORATE: A Program for Direct Dynamics Calculations of Chemical Reaction Rates by Semiempirical Molecular Orbital Theory. *Comput. Phys. Commun.* **1993**, *75*, 143−159.
(44) Liu, Y.-P.; Lu, D.h.; Gonzalez-Lafont, A.; Truhlar, D. G.; Garrett, B. C. Direct Dynamics Calculation of the Kinetic Isotope Effect for an Organic Hydrogen-Transfer Reaction, Including Corner-Cutting Tunneling in 21 Dimensions. *J. Am. Chem. Soc.* **1993**, *115*, 7806−7817.
(45) Liu, Y.-P.; Lynch, G. C.; Truong, T. N.; Lu, D.h.; Truhlar, D. G. Molecular Modeling of the Kinetic Isotope Effect for the [1,5]-Sigmatropic Rearrangement of cis-1,3-Pentadiene. *J. Am. Chem. Soc.* **1993**, *115*, 2408−2415.
(46) Fernandez-Ramos, A.; Truhlar, D. G. Improved Algorithm for Corner Cutting Calculations. *J. Chem. Phys.* **2001**, *114*, 1491−1496.
(47) Garrett, B. C.; Truhlar, D. G. A Least-Action Variational Method for Calculating Multi-dimensional Tunneling Probabilities for Chemical Reactions. *J. Chem. Phys.* **1983**, *79*, 4931−4938.
(48) Meana-Pañeda, R.; Truhlar, D. G.; Fernandez-Ramos, A. Least-Action Tunneling Transmission Coefficient for Polyatomic Reactions. *J. Chem. Theor. Comput.* **2010**, *6*, 6−17.
(49) Zheng, J.; Zhang, S.; Lynch, B. J. Corchado, J. C.; Chuang, Y.-Y.; Fast, P. L.; Hu, W.-P.; Liu, Y.-P.; Lynch, G. C.; Nguyen, K. A.; TruhlarD. G.; et al. *POLYRATE-2010-A*; University of Minnesota: Minneapolis, MN, 2010.
(50) Suleimanov, Y. V.; Allen, J. W.; Green, W. H. RPMDRATE: Bimolecular Chemical Reaction Rates from Ring Polymer Molecular Dynamics. *Comput. Phys. Commun.* **2013**, *184*, 833−840.
(51) Li, Y.; Suleimanov, Y. V.; Yang, M.; Green, W. H.; Guo, H. Ring Polymer Molecular Dynamics Calculations of Thermal Rate Constants for the $O(^3P) + CH_4 \rightarrow OH + CH_3$ Reaction: Contributions of Quantum Effects. *J. Phys. Chem. Lett.* **2013**, *4*, 48−52.
(52) Li, Y.; Suleimanov, Y. V.; Li, J.; Green, W. H.; Guo, H. Rate Coefficients and Kinetic Isotope Effects of the $X + CH_4 \rightarrow CH_3 + HX$ (X = H, D, Mu) Reactions from Ring Polymer Molecular Dynamics. *J. Chem. Phys.* **2013**, *138*, 094307.
(53) Suleimanov, Y. V.; Pérez de Tudela, R.; Jambrina, P. G.; Castillo, J. F.; Sáez-Rábanos, V.; Manolopoulos, D. E.; Aoiz, F. J. A Ring Polymer Molecular Dynamics Study of the Isotopologues of the $H + H_2$ Reaction. *Phys. Chem. Chem. Phys.* **2013**, *15*, 3655−3665.

(54) Suleimanov, Y. V. Surface Diffusion of Hydrogen on Ni(100) from Ring Polymer Molecular Dynamics. *J. Phys. Chem. C* **2012**, *116*, 11141−11153.
(55) Allen, J. W.; Green, W. H.; Li, Y.; Guo, H.; Suleimanov, Y. V. Communication: Full Dimensional Quantum Rate Coefficients and Kinetic Isotope Effects from Ring Polymer Molecular Dynamics for a Seven-Atom Reaction OH + CH_4 –> CH_3 + H_2O. *J. Chem. Phys.* **2013**, *138*, 221103.
(56) Pérez de Tudela, R.; Suleimanov, Y. V.; Menendez, M.; Castillo, F.; Aoiz, F. J. A Ring Polymer Molecular Dynamics Study of the Cl + O_3 Reaction. *Phys. Chem. Chem. Phys.* **2014**, *16*, 2920−2927.
(57) Espinosa-Garcia, J.; Fernandez-Ramos, A.; Suleimanov, Y. V.; Corchado, J. C. Theoretical Study of the F(^{2}P) + NH_3 Hydrogen Abstraction Reaction: Mechanism and Kinetics. *J. Phys. Chem. A* **2014**, *118*, 554−560.
(58) Li, Y.; Suleimanov, Y. V.; Green, W. H.; Guo, H. Quantum Rate Coefficients and Kinetic Isotope Effect for the Reaction Cl + CH_4 → HCl + CH_3 from Ring Polymer Molecular Dynamics. *J. Phys. Chem. A* **2014**, *118*, 1989−1996.
(59) Li, Y.; Suleimanov, Y. V.; Guo, H. Ring-Polymer Molecular Dynamics Rate Coefficient Calculations for Insertion Reactions: X + H_2 → HX + H (X═N, O). *J. Phys. Chem. Lett.* **2014**, *5*, 700−705.
(60) Klippenstein, S. J.; Allen, W. D. Variable reaction coordinate direct RRKM theory. *Ber. Bunsen-Ges. Phys. Chem.* **1997**, *101*, 423−437.
(61) Sanson, J. A.; Sanchez, M. L.; Corchado, J. C. Importance of Anharmonicity, Recrossing Effects, and Quantum Mechanical Tunneling in Transition State Theory with Semiclassical Tunneling. A Test Case: The H_2 + Cl Hydrogen Abstraction Reaction. *J. Phys. Chem. A* **2006**, *110*, 589−599.
(62) Garrett, B. C.; Truhlar, D. G. WKB approximation for the eactiopn-path Hamiltonian: Application to variational transition state theory, vibrationaly adiabatic excited-state barrier heights, and resonance calculations. *J. Chem. Phys.* **1984**, *81*, 309−317.
(63) Isaacson, A. D. Including anharmonicity in the calculation of rate constants. 1. The HCN/HNC isomerization reaction. *J. Phys. Chem. A* **2006**, *110*, 379−388.
(64) Isaacson, A. D. Including anharmonicity in the calculation of rate constants. II. The OH+ H2 → H2 O+H reaction. *J. Chem. Phys.* **2008**, *128*, 134304.
(65) Chase, M. W.; Davis, C. A.; Downey, J. R.; Frurip, D. J.; McDonald, R. A.; Syverud, A. N. JANAF Thermochemical Tables. *J. Phys. Chem. Ref. Data* **1985**, Suppl. 14.